# Comments on "Satellite Observations of a Severe Supercell Thunderstorm on 24 July 2000 Made during the *GOES-11* Science Test"

BRIAN A. KLIMOWSKI AND MATTHEW J. BUNKERS

*NOAA/NWS Weather Forecast Office, Rapid City, South Dakota*

14 March 2002 and 20 May 2002

## 1. Introduction

Weaver et al. (2002, hereinafter W02) presented a case study in which *Geostationary Operational Environmental Satellite-11* (*GOES-11*) rapid-scan imagery and sounder data were examined for their effectiveness in providing short-range forecasts of the development and evolution of a tornadic supercell over South Dakota and Nebraska on 24 July 2000. We agree with W02 that the *GOES-11* imagery data were useful in highlighting a decaying mesoscale convective system (MCS) and its resultant low-level thunderstorm outflow (LTO). Furthermore, the *GOES-11* sounder data provided insight into the spatial extent of an instability axis and the corresponding convective inhibition and also served as a cross-reference check to numerical model instability forecasts. We appreciate the efforts of W02 to bring attention to these valuable forecasting data.

Even though the focus of W02's paper is on satellite observations, they did discuss aspects of supercell evolution, and we would like to comment on and clarify some of these statements. In particular, the importance of the relationship between vertical wind shear and supercell formation and motion was not addressed, and, furthermore, none of the readily available supercell motion forecast techniques were considered. Rather, satellite data were emphasized in their discussion of supercell processes in lieu of other relevant data sources. Conclusions were drawn about both the right- and left-moving supercells based mostly on satellite data, when radar data and severe-storm reports showed a much different picture of their evolutions. Therefore, we comment here on W02's paper to describe (i) how the 24 July 2000 supercell *evolution* (formation and motion) can be readily explained through a vertical wind shear perspective and existing techniques to forecast supercell motion, (ii) the benefits of using all available data sources to assess the convective environment and thunderstorm evolution, and (iii) the pitfalls of focusing too much on a single data source.

## 2. Supercell formation and motion related to vertical wind shear

Much has been learned about supercell dynamics over the last several decades (e.g., Klemp 1987; Weisman and Rotunno 2000). It has generally been accepted that supercells develop when an updraft of sufficient strength interacts with ambient vertical wind shear of sufficient magnitude to promote both rotation and an upward-directed pressure gradient force on the storm's flanks. This leads to splitting supercells—one that rotates counterclockwise (clockwise) and moves to the right (left) of the vertical wind shear. In addition, clockwise (counterclockwise) turning of the low-level shear vectors preferentially favors the right- (left) moving storm. Modeling (e.g., Weisman and Rotunno 2000) and observational (e.g., Bunkers et al. 2000; Bunkers 2002) studies both indicate that 0–6-km total (bulk) wind shear[1] of 20–25 (10–15) m $s^{-1}$ is necessary for supercell processes to occur (one may prefer to use 0–5- or 0–7-km layers instead, with slightly different shear values, of course). Moreover, vertical wind shear (either total or bulk) has been recognized recently as a more robust parameter for anticipating the general shear requirements for supercell development—as opposed to storm-relative helicity (SRH), which often exhibits considerable temporal and spatial variability (e.g., Markowski et al. 1998). Capitalizing on the above information, Rasmussen and Blanchard (1998) and Bunkers et al. (2000)

*Corresponding author address:* Dr. Brian A. Klimowski, NOAA/NWS Weather Forecast Office, 300 East Signal Dr., Rapid City, SD 57701-3800.
E-mail: brian.klimowski@noaa.gov

[1] The 0–6-km bulk wind shear is typically represented by the vector difference between the surface and 6-km winds. The 0–6-km total (also-called cumulative) wind shear [similar to mean shear; Rasmussen and Wilhelmson (1983)] is represented by a summation of the shear segments across shallow sublayers (e.g., 500-m depth) from 0 to 6 km. Total wind shear is a measure of hodograph length.

presented techniques to predict supercell motion based on the vertical wind shear.

### a. Sufficient vertical wind shear for supercell formation

Given the present understanding of supercell formation processes related to the vertical wind shear, we find disagreement with W02's (p. 131) statement regarding shear from the 1200 UTC 24 July 2000 North Platte, Nebraska, (LBF)[2] sounding:

> The backing and intensifying winds would increase the *marginally favorable shear* [the 0–3-km storm relative environmental helicity (SREH) from the morning sounding was 122 $m^2 s^{-2}$]. [Italics added.]

Based on the 1200 (0000) UTC 24 (25) July 2000 soundings from LBF, the 0–6-km total wind shear was 53 (41) $m s^{-1}$, which is 2 times the minimum shear required for supercell processes to occur (see previous paragraph).[3] This shear environment was clearly favorable for supercells, with values near the 75th percentile of the distribution from Bunkers et al. (2000, their Fig. 3a). Even though both of these soundings resulted in an observed 0–3-km SRH from 95 to 125 $m^2 s^{-2}$, Bunkers et al. (2000, their Fig. 3b) showed about one-third of their supercell cases had SRH of less than 125 $m^2 s^{-2}$, which is consistent with the values herein. This result highlights a common pitfall of using SRH for forecasting general supercell occurrence, because values may be lower than what has been traditionally considered sufficient for supercell development to occur. *In summary, this was a moderately sheared environment, which favored the development of supercells.*

### b. Supercell motion related to vertical wind shear

It is interesting that W02 discussed possible causes of supercell motion but did not mention well-known techniques that anticipate supercell motion (i.e., Maddox 1976; Colquhoun 1980; Davies and Johns 1993; UCAR 1996; Davies 1998; Rasmussen and Blanchard 1998; Bunkers et al. 2000). For example, W02 (p. 135) stated:

> Notice that the storm—which was moving from about 350°—seemed to have been propagating along the axis of highest CAPE, which, in turn, was situated along and near the north–south convergence boundary. Furthermore, the path of the most intense new development coincided with a narrow tongue of eroding CIN as computed from the same half-hourly sounder data (Fig. 11). *It is possible that the storm was propagating south along this convergence boundary with new updrafts growing at the leading edge of its own outflow* in a manner similar to that described by Weaver and Nelson (1982). Animated reflectivity data show new towers growing in a quasi-discrete fashion ahead of the most intense cores (e.g., Fig. 12). [Italics added; CIN is convective inhibition.]

A little later on, W02 (p. 136) suggested,

> These data show that *the right-mover's motion could readily be explained by factors other than shear-induced pressures,* though the effects of the shear cannot be eliminated. [Italics added.]

It is already clear from section 2a that sufficient vertical wind shear existed for supercells on this day; therefore, it is unclear why shear-induced pressures would not have played a major role in governing supercell formation and motion. A radar analysis of the splitting storms from development to the weakening stages suggests the right-moving supercell of interest had long periods of steady, consistent motion (Table 1, Fig. 1). Most of the apparent discrete development occurred during the first 93 min of the supercell's lifetime (2207–2340 UTC), but a close examination of radar data indicated that this development consisted of feeder cells

TABLE 1. Summary of pertinent radar-observed stages for the splitting thunderstorms on 24–25 Jul 2000 over south-central South Dakota and central Nebraska. The storm motion was computed by tracking the thunderstorm centroids from the lowest-level reflectivity scans. Here RM denotes right-moving supercells, and LM denotes left-moving supercells.

| Time (UTC) | Storm motion | Notes |
|---|---|---|
| 2141–2207 | | Thunderstorm displayed a classical split |
| 2207–2340 | 348°/18 kt | RM1; two feeder cells noted on southwestern flank; a secondary mesocyclone formed around 2300 UTC |
| 2340–0040 | 355°/22 kt | RM1; one strong persistent mesocyclone; classic structure |
| 0040–0140 | 355°/22 kt | RM1; one strong persistent mesocyclone; classic structure |
| 0140–0400 | 344°/26 kt | RM1; one strong persistent mesocyclone; high-precipitation structure; a few feeder cells noted on southern flank |
| 0400–0630 | 323°/22 kt | RM1; *interacted* with other convection; storm eventually lost identity and weakened |
| 2207–2248 | 241°/12 kt | LM1; intensified rapidly but was relatively short lived |
| 2254–2319 | | New thunderstorm developed on outflow of LM1 and then split again |
| 2319–0007 | 318°/15 kt | RM2; much weaker and shorter lived than RM1 |
| 2319–0007 | 245°/15 kt | LM2; weaker than LM1 |

[2] Instead of use of the 1200 UTC LBF sounding to anticipate the afternoon/evening shear profile, we believe vertical wind profiles both from radar networks and from profiler networks, along with model forecast soundings and surface data, would have been more beneficial in assessing the shear environment.

[3] Moreover, the 0–6-km bulk shear was 23.7 (26.3) $m s^{-1}$ from the 1200 (0000) UTC LBF soundings, which again is 2 times the minimum values typically observed in supercell environments (e.g., Bunkers 2002).

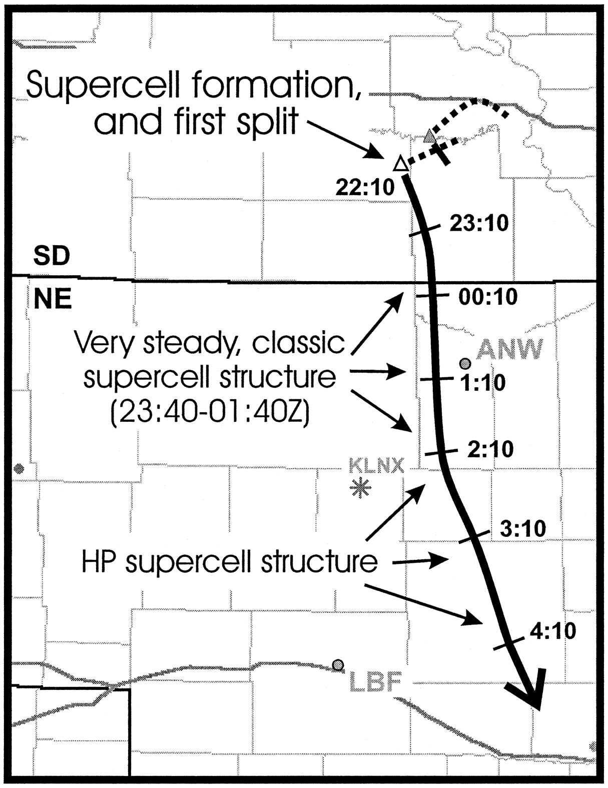


FIG. 1. Selected storm tracks for 24–25 Jul 2000 (all times UTC). The supercell of interest (RM1; see Table 1) corresponds to the long solid line with time markings. A second, short-lived, right-moving supercell is indicated with the short solid line. The short dashed lines correspond to two short-lived left-moving supercells. The location of the first thunderstorm split is marked with an open triangle, and the second split is noted with a filled triangle.

[as described by Browning (1977), 4–5] merging onto the western flanks of the main storm. The mesocyclone, determined from storm-relative velocity data, experienced only one regeneration during this time [similar to that described in Burgess et al. (1982)] but was otherwise persistent throughout this period and apparently never propagated in a discrete manner. Furthermore, the storm motion was steady in a southerly direction. Therefore, this initial period did not appear to be dominated by discrete development caused by boundary layer convergence as W02 claimed [and as described in Weaver and Nelson (1982)].

The next stage consisted of a 2-h period of steady motion (2340–0140 UTC) during which the supercell was very intense (displaying a hook echo and bounded weak-echo region), and was considered to be classic (CL; Moller et al. 1994). No discrete development was noted during this stage, and the storm motion was slightly faster than that in the previous stage (cf. 2207–2340 with 2340–0140 UTC in Table 1). The fact that the motion was slightly farther to the right of the shear is consistent with the stronger mesocyclone and, hence, stronger shear-induced pressures. The supercell eventually evolved into a high-precipitation storm (HP; Moller et al. 1994), at which time its speed increased slightly (0140–0400 UTC in Table 1). These observations are consistent with both the tendency for CL supercells to make a transition to HP supercells (Moller et al. 1994) and the tendency for the cold pool to become increasingly dominant with time (e.g., UCAR 1996). *In summary, radar observations revealed a relatively steady and coherent evolution of this supercell and its attendant mesocyclone, consistent with the theory of continuous propagation caused by rotationally induced nonhydrostatic vertical pressure gradients (e.g., Rotunno and Klemp 1985).*

Using a Rapid Update Cycle (RUC) model analysis sounding for the site just downstream of the supercell at 0000 UTC 25 July 2000 (Ainsworth, Nebraska; ANW[4]—see Fig. 1 for the location), the observed motion of the right-moving supercell compared favorably to that predicted by the shear-relative method of Bunkers et al. (2000; our Fig. 2a). The hodograph also reveals that (i) the SRH was probably higher near the location of the supercell (289 $m^2$ $s^{-2}$), which was coincident with the storm's tornadic phase; (ii) clockwise curvature of the shear vectors in the low levels was present, which favored the right-moving supercell over the left-mover (refer back to Table 1, Fig. 1); and (iii) it is beneficial to consult all available data sources to ascertain the convective environment, because the LBF sounding did not reveal SRH of this magnitude (cf. Figs. 2a and 2b). As the storm moved closer to LBF during 0140–0400 UTC (Fig. 1), the observed supercell motion, which had shifted slightly to the left, was also similar to the predicted motion obtained from the observed LBF hodograph (Fig. 2b). This information can alternatively be observed in plan view by superimposing the forecast supercell motion derived from a coarse 80-km grid of the RUC model with the radar data (e.g., Fig. 3). Although not perfect, it is readily apparent that the vertical wind shear perspective provided adequate information regarding the motion of this storm. Plotting the anticipated motion of supercells over the animated radar data in this way has been found to be operationally useful for the identification and forecasting of supercell thunderstorms.

When combining information from the *GOES-11* dataset (W02) with the radar and kinematic data herein, one gets a more complete picture of the supercell evolution. First, the storm moved in a direction that is consistent with updraft–shear interactions: propagation to the right of the environmental shear. Second, radar and satellite data both showed brief periods of quasi-discrete development, but the radar data also indicated that continuous propagation was the dominant mode as the

[4] The 0000 UTC 25 July 2000 observed LBF sounding compared favorably to the RUC analysis for LBF, so we believe this RUC analysis hodograph at ANW is representative of the large-scale environment at ANW.

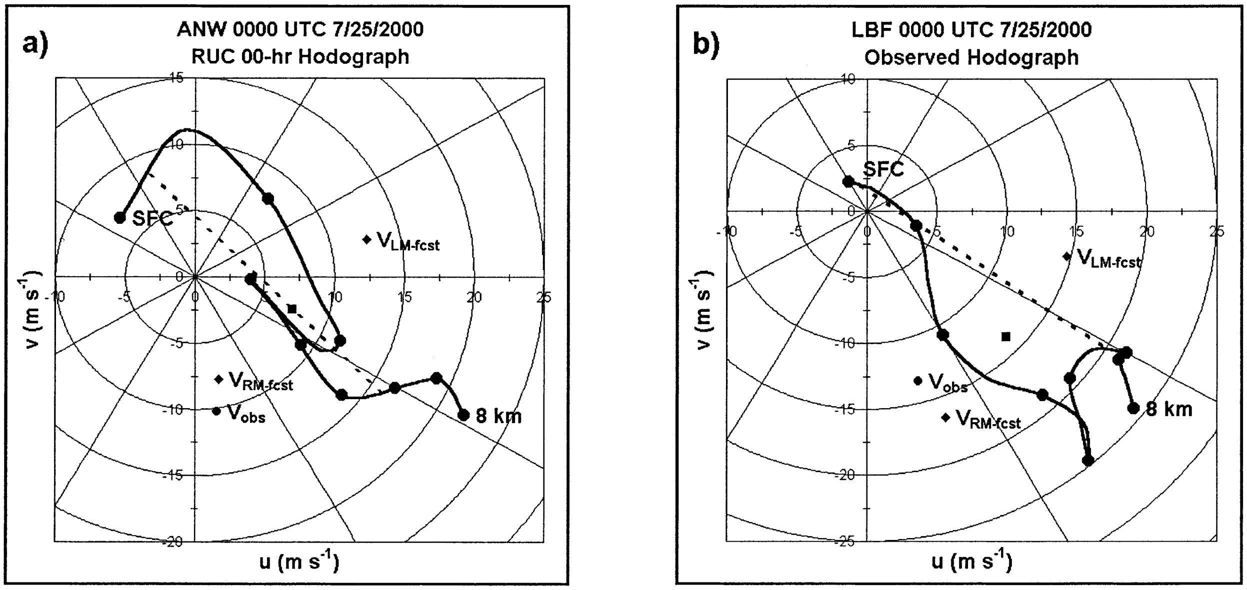


FIG. 2. The 0–8-km hodographs for (a) Ainsworth, NE (ANW), using the RUC analysis, and (b) North Platte, NE (LBF), using the observed sounding. Points are plotted at 500-m increments AGL, with filled circles at 1-km intervals AGL. The observed storm motions are plotted for the right-moving supercell ($V_{obs}$), the forecast supercell motions are plotted for left- ($V_{LM\text{-}fcst}$) and right-moving ($V_{RM\text{-}fcst}$) supercells using the method of Bunkers et al. (2000), the 0–6-km mean wind is indicated with a filled square, and the shear from the boundary layer to 6 km is represented with a dashed line.

storm evolved from CL to HP. Third, the higher SRH seen in Fig. 2a, combined with the flanking towers seen in the *GOES-11* imagery (W02, 136–137), supported a higher probability of tornadogenesis near the South Dakota–Nebraska border (three tornadoes were reported in this area). Fourth, the forecast supercell motion, which was coincident with the instability axis identified with the *GOES-11* and numerical model data, favored a long-lived supercell. Indeed, we believe it was the coincidence of the instability axis and the shear-related supercell motion that favored the longevity of the storm, rather than what W02 purport, namely, that the supercell moved south because of the existence of the instability axis. Furthermore, the vertical wind shear (see dashed lines in Fig. 2) was oriented approximately 135° to the right of the north–south convergence axis—a favorable arrangement for a long-lived southeastward-moving cyclonic supercell (Bluestein and Weisman 2000, their Figs. 4 and 9d). *In summary, we believe that updraft–shear interactions satisfactorily explained the supercell motion in a scientifically sound manner and that shear-induced pressures were not negligible as implied by W02.*

## 3. Observations of the splitting storms

Although W02 showed how the *GOES-11* data can be very useful for monitoring boundaries, convective initiation, and the spatial extent of instability, we believe they downplayed the importance of radar data, which in turn led them to questionable conclusions about storm development and longevity, especially with regard to the left-moving supercells.

### *Classical splitting signatures and the left-moving storms*

W02 (133–134) suggested that the supercell formation did not follow the ''classical'' storm split process, and they also made claims, based on satellite data, that cannot be substantiated with an analysis of radar data:

> Data from the NWS Weather Surveillance Radar-1988 Doppler (WSR-88D) at Thedford, Nebraska, show this split clearly (Fig. 8). However, *satellite imagery reveals that the process may not have been a ''classical'' storm split, that is, one in which shear-induced pressure gradients on the flanks of the original updraft enhance lift, thereby producing two new updrafts* (e.g., Rotunno and Klemp 1982, 1985). Figure 9, and especially sequential visible imagery, show that the left-moving component in this case appears to have formed along a northward moving outflow boundary. Also, the imagery shows that when the new cell intersected the old LTO boundary that was associated with the MCS (discussed in section 4), it intensified discernibly and began moving east along the associated cloud line. Note that the hodograph was curved cyclonically in this case (Fig. 3). With this type of hodograph, in a classical storm-splitting situation, one should expect a region of high pressure to develop above the low pressure area on the left flank, causing the left-moving updraft to quickly dissipate (Wilhelmson and Klemp 1981). In this case, the left-mover did not dissi-

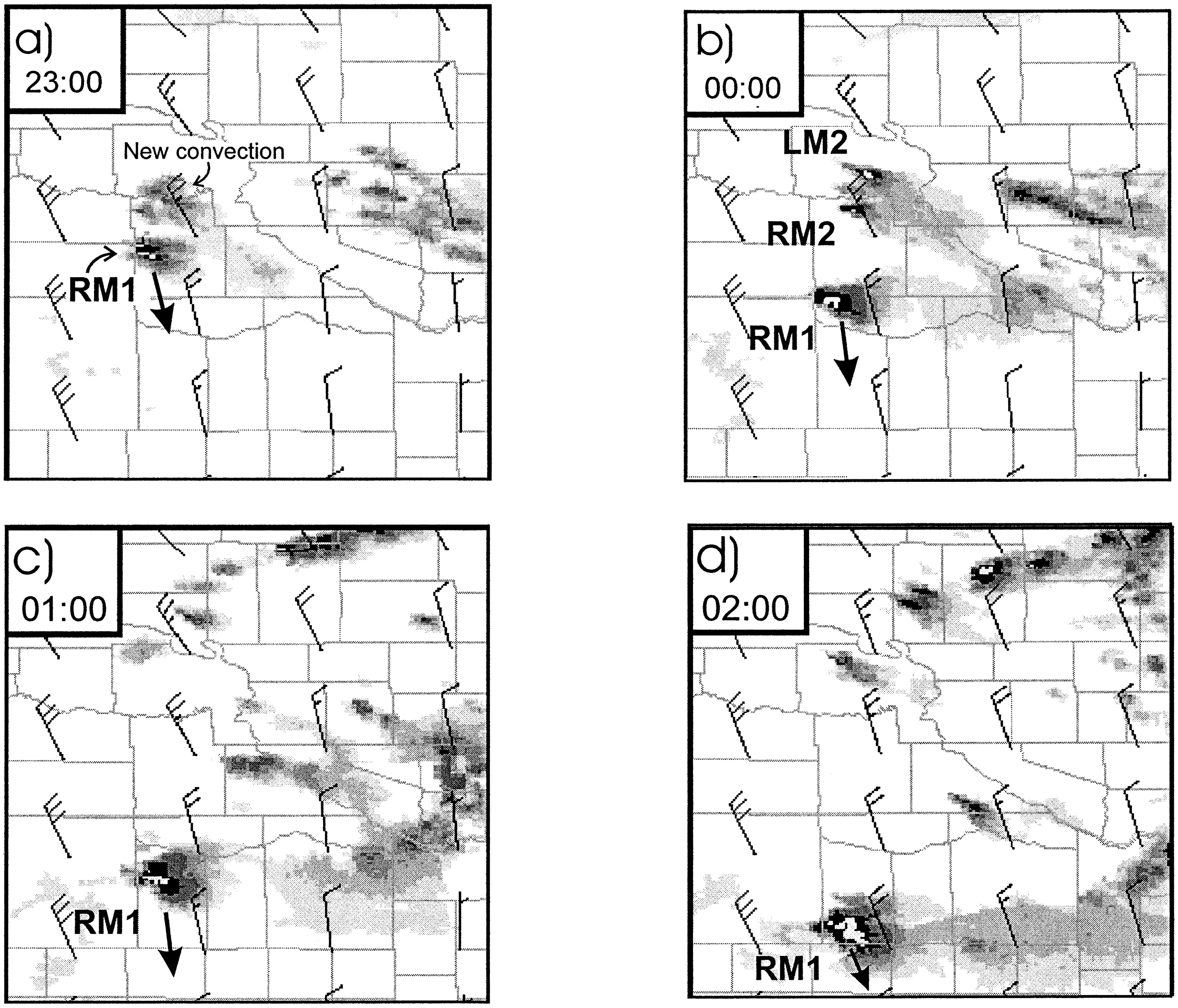


FIG. 3. Radar reflectivity images for (a) 2300 UTC 24 Jul, (b) 0000 UTC 25 Jul, (c) 0100 UTC 25 Jul, and (d) 0200 UTC 25 Jul 2000. Forecast supercell motion vectors derived from the 0000 UTC 25 Jul 2000 RUC model are superimposed on (a), (b), and (c), with 0300 UTC RUC model data superimposed on (d). Here RM denotes right-moving supercells, and LM denotes left-moving supercells. Dark arrows indicate the relative motion of RM1.

> pate, but continued east along the preexisting convergence line for more than 2 h and produced severe weather all along its path. It appeared to travel along the LTO boundary that had been created by the MCS earlier in the day in a manner similar to that discussed by Weaver (1979). [Italics added.]

We have several points of contention with these statements. First, we disagree with W02's implication that one can use satellite data to infer rotational characteristics about supercells. Instead, radar data confirm that this was indeed a classical storm-splitting process. Storm-relative velocity data lucidly show that cyclonic and anticyclonic velocity couplets were associated with the initial splitting thunderstorm (Fig. 4). At 2141 UTC, the initial thunderstorm was widening and displayed clockwise (counterclockwise) rotation on its northern (southern) flanks (Figs. 4a and 4c). By 2207 UTC, the thunderstorm had almost completed its split, and the circulations remained on the storm flanks as previously described (Figs. 4b and 4d). The cyclonic circulation persisted with the right-moving supercell for several hours, whereas the left-moving supercell dissipated after about 45 min (refer to Table 1). Furthermore, the reflectivity data indicate that the splitting process evolved in a manner similar to the sequence of events described in Achtemeier (1969). According to these data, the left-moving storm did not develop separately along a northward moving outflow boundary as W02 stated. This sequence of events followed the prototypical development process for supercells [Weisman and Rotunno (2000, p. 1453); also refer to the beginning of section 2], which could not be deduced from the satellite im-

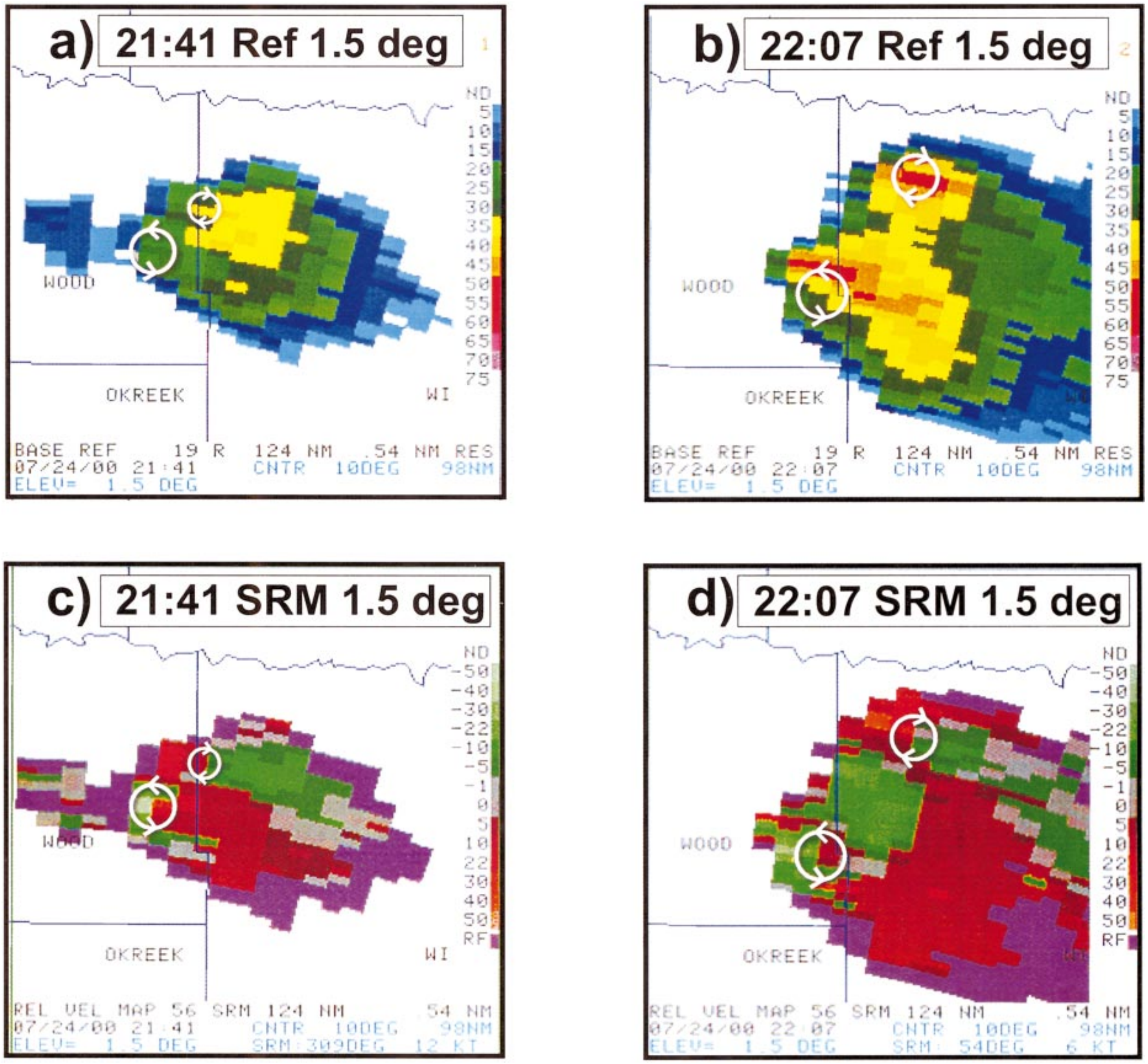


FIG. 4. Thedford, NE (KLNX), 1.5° slice radar images on 24 Jul 2000 for (a) 2141 UTC reflectivity, (b) 2207 UTC reflectivity, (c) 2141 UTC storm-relative velocity, and (d) 2207 UTC storm-relative velocity. White circles are used to denote the sense of rotation.

agery. Second, *radar data did not show* that the first left-moving supercell intersected an old LTO boundary, intensified, and then persisted for more than 2 h as it moved east (as W02 claimed). Moreover, it did not result in any reported severe weather (NCDC 2000). This first left-moving supercell dissipated about 45 min after it split (Table 1; Fig. 1, open triangle), and, in addition, the anticyclonic circulation was weaker than that of its right-moving counterpart. After this first left-moving supercell dissipated shortly before 2300 UTC, a second thunderstorm formed on its outflow (Fig. 3a) and then split again (Table 1; Fig. 1, filled triangle; Fig. 3b). This second split is likely what W02 inferred from the *GOES-11* visible imagery, although it occurred about 15 min later than the time of the image in their Fig. 9. Furthermore, the second left-moving supercell was also short lived and was associated with only one severe-weather report. This example illustrates a case in which satellite data led W02 to faulty conclusions and indicates that a closer inspection of the radar data and severe-storm reports was warranted.

The ANW hodograph (Fig. 2a) favored a dominant right-moving supercell given the clockwise turning of the low-level shear vectors, with suppression of left-moving storms. This vertical wind shear profile supports the relatively rapid dissipation of the left-moving storms, as well as their relatively weaker circulations, which was observed on this day. In addition, there were at least two short-lived (10–20 min) anticyclonic circulations noted on the northern flank of the long-lived right-moving supercell during its early stages. A misinterpretation of the satellite data, combined with the lack of a detailed radar and severe-storm-report analysis, led W02 to conclude mistakenly that shear-induced pressures were not significant for the left-moving storms. *In summary, two relatively weak and short-lived left-moving storms occurred on this day, both of which evolved from a storm-splitting process consistent with the environmental hodograph. The second left-moving storm produced one severe-weather report.*

## 4. Final remarks

Based on our above comments regarding W02, the following summary statements are made:

1) Updraft–shear interactions provide a simple and scientifically sound explanation for the supercell development and motion on 24 July 2000.
2) It is beneficial to make thorough use of all available data sources when examining both the convective environment and thunderstorm evolution, and overreliance on any single data source should be avoided.
3) Care must be exercised when observing thunderstorm motion in order to examine the effects of continuous propagation (shear induced) versus discrete propagation (external factors).
4) The simultaneous display of radar reflectivity data with both the mean wind and forecast supercell motion can enhance the ability of forecasters to identify developing supercells.

We want to reiterate and to applaud the main theme of W02, that is, satellite data can be of significant value in the operational forecasting/warning setting of severe convective storms. However, one must *carefully* consider all available data sources and not put too much weight on any one data source.

*Acknowledgments.* We are grateful to John Stoppkotte (Science and Operations Officer, NWS North Platte, Nebraska), for providing archive-IV radar data from Thedford, Nebraska, (KLNX) and to John Stoppkotte and Jon Zeitler (Forecaster, NWS Houston/Galveston, Texas) for reviewing the manuscript. We also thank David Carpenter (Meteorologist-in-Charge, NWS Rapid City, South Dakota) for supporting this work.

REFERENCES

Achtemeier, G. L., 1969: Some observations of splitting thunderstorms over Iowa on August 25–26, 1965. Preprints, *Sixth Conf. on Severe Local Storms,* Chicago, IL, Amer. Meteor. Soc., 89–94.

Bluestein, H. B., and M. L. Weisman, 2000: The interaction of numerically simulated supercells initiated along lines. *Mon. Wea. Rev.,* **128,** 3128–3149.

Browning, K. A., 1977: The structure and mechanisms of hailstorms. *Hail: A Review of Hail Science and Hail Suppression, Meteor. Monogr.,* No. 38, Amer. Meteor. Soc., 1–43.

Bunkers, M. J., 2002: Vertical wind shear associated with left-moving supercells. *Wea. Forecasting,* **17,** 845–855.

——, B. A. Klimowski, J. W. Zeitler, R. L. Thompson, and M. L. Weisman, 2000: Predicting supercell motion using a new hodograph technique. *Wea. Forecasting,* **15,** 61–79.

Burgess, D. W., V. T. Wood, and R. A. Brown, 1982: Mesocyclone evolution statistics. Preprints, *12th Conf. on Severe Local Storms,* San Antonio, TX, Amer. Meteor. Soc., 422–424.

Colquhoun, J. R., 1980: A method of estimating the velocity of a severe thunderstorm using the vertical wind profile in the storm's environment. Preprints, *Eighth Conf. on Weather Forecasting and Analysis,* Denver, CO, Amer. Meteor. Soc., 316–323.

Davies, J. M., 1998: On supercell motion in weaker wind environments. Preprints, *19th Conf. on Severe Local Storms,* Minneapolis, MN, Amer. Meteor. Soc., 685–688.

——, and R. H. Johns, 1993: Some wind and instability parameters associated with strong and violent tornadoes. Part I: Wind shear and helicity. *The Tornado: Its Structure, Dynamics, Prediction, and Hazards, Geophys. Monogr.,* No. 79, Amer. Geophys. Union, 573–582.

Klemp, J. B., 1987: Dynamics of tornadic thunderstorms. *Annu. Rev. Fluid Mech.,* **19,** 369–402.

Maddox, R. A., 1976: An evaluation of tornado proximity wind and stability data. *Mon. Wea. Rev.,* **104,** 133–142.

Markowski, P. M., J. M. Straka, E. N. Rasmussen, and D. O. Blanchard, 1998: Variability of storm-relative helicity during VORTEX. *Mon. Wea. Rev.,* **126,** 2959–2971.

Moller, A. R., C. A. Doswell III, M. P. Foster, and G. R. Woodall, 1994: The operational recognition of supercell thunderstorm environments and storm structures. *Wea. Forecasting,* **9,** 327–347.

NCDC, 2000: *Storm Data.* Vol. 42, No. 7, 318 pp. [Available from National Climatic Data Center, 151 Patton Ave., Asheville, NC 28801-5001.]

Rasmussen, E. N., and R. B. Wilhelmson, 1983: Relationships between storm characteristics and 1200 GMT hodographs, low-level shear, and stability. Preprints, *13th Conf. on Severe Local Storms,* Tulsa, OK, Amer. Meteor. Soc., J5–J8.

——, and D. O. Blanchard, 1998: A baseline climatology of sounding-derived supercell and tornado forecast parameters. *Wea. Forecasting,* **13,** 1148–1164.

Rotunno, R., and J. B. Klemp, 1982: The influence of the shear-induced pressure gradient on thunderstorm motion. *Mon. Wea. Rev.,* **110,** 136–151.

——, and ——, 1985: On the rotation and propagation of simulated supercell thunderstorms. *J. Atmos. Sci.,* **42,** 271–292.

UCAR, 1996: *Anticipating Convective Storm Structure and Evolution.* Cooperative Program for Operational Meteorology, Education, and Training, University Corporation for Atmospheric Research, CD-ROM. [Available from COMET, P.O. Box 3000, Boulder, CO 80307-3000.]

Weaver, J. F., 1979: Storm motion as related to boundary-layer convergence. *Mon. Wea. Rev.,* **107,** 612–619.

——, and S. P. Nelson, 1982: Multiscale aspects of thunderstorm gust fronts and their affects on subsequent storm development. *Mon. Wea. Rev.,* **110,** 707–718.

——, J. A. Knaff, D. Bikos, G. S. Wade, and J. M. Daniels, 2002: Satellite observations of a severe supercell thunderstorm on 24 July 2000 made during the *GOES-11* science test. *Wea. Forecasting,* **17,** 124–138.

Weisman, M. L., and R. Rotunno, 2000: The use of vertical wind shear versus helicity in interpreting supercell dynamics. *J. Atmos. Sci.,* **57,** 1452–1472.

Wilhelmson, R. B., and J. B. Klemp, 1981: A three-dimensional numerical simulation of splitting severe storms on 3 April 1964. *J. Atmos. Sci.,* **38,** 1581–1600.